NUCL SCI TECH (2017) 28:82
DOI 10.1007/s41365-017-0235-6

Theoretical study of the interaction between hydrogen and 4*d* alloying atom in nickel

Wen-Guan Liu[1] · Yuan Qian[1] · Dong-Xun Zhang[1] · Xing-Bo Han[1] · Xin-Xin Chu[1] · You-Shi Zeng[1] · Guang-Liang Bao[1] · Guang-Hua Wang[1] · Sheng-Wei Wu[1] · Wei Liu[1]

Received: 21 October 2016 / Revised: 23 December 2016 / Accepted: 19 January 2017 / Published online: 6 May 2017

Abstract In order to investigate the tritium behaviors in Hastelloy N alloy in molten salt reactor, first-principles calculations are used to study the interaction between hydrogen and 4*d* transition metal alloying atom in nickel-based alloy. The interaction energies between 4*d* elements and H are calculated. Atomic size effects and electron distribution effects are analyzed. The hydrogen–4*d* interactions are compared with the hydrogen–3*d* interactions calculated in our previous work.

Keywords Hydrogen · Tritium · Transition metal · Nickel · First-principles calculation

1 Introduction

Hastelloy N, a Ni-based alloy, is the special structural material for molten salt reactor (MSR) [1, 2] with excellent corrosion resistance against molten salts. Tritium (T), produced by neutron reactions with FLiBe molten salt, can flow readily through the Hastelloy N walls of various systems in MSR. With radioactivity, T release to the environment must be controlled. Knowledge of H behavior in Ni-based alloy is essential for predicting T behavior in MSR and guiding T control processes [3]. Also, H behavior in alloys is a fundamental subject for understanding hydrogen embrittlement [4, 5] suffered by alloys.

While it is difficult to experimentally explore H behaviors in alloys, first-principles calculations can be used to study H behaviors in alloys and their underlying physical mechanisms at the atomic and electronic levels [6, 7]. Since the alloying additives can directly modify H behavior in alloys, the interactions between them are very important.

In our previous first-principles calculations [8], the interactions between H and 3*d* transition metal (TM) alloying atom in Ni were found to be influenced greatly by the electron distribution, which do not obey the elastic mechanism [9] or the “reverse stability” rule [10]. In this work, we further investigated the interaction between 4*d* TM atoms and H in Ni with first-principles calculations, and the differences between 4*d* and 3*d* elements in their interaction with H.

2 Computational details

The computational method is stated in detail in our previous work [8], and spin-polarized electronic state calculations are performed within the density functional theory [11, 12] using Vienna ab initio simulation package (VASP) [13]. A 2 × 2×2 Ni supercell containing 32 Ni atoms is used with a Monkhorst–Pack 7 × 7×7 k-point mesh. In the Ni–4*d* supercell, a Ni atom is replaced by a

---

This work was supported by the “Strategic Priority Research Program” of the Chinese Academy of Sciences (No. XDA02020200), and the National Natural Science Foundation of China (No. 51601212).

✉ Wen-Guan Liu
liuwenguan@sinap.ac.cn

✉ Wei Liu
liuwei@sinap.ac.cn

Guang-Liang Bao
baoguangliang@sinap.ac.cn

Sheng-Wei Wu
wushengwei@sinap.ac.cn

[1] Shanghai Institute of Applied Physics, Chinese Academy of Sciences, Shanghai 201800, China

4*d* atom. In the Ni–4*d*–H supercell, one H atom is placed in the octahedral or tetrahedral interstitial site (O-site or T-site) nearest to the substitutional 4*d* atom. Energies of H vibrations are taken into account by calculating the zero-point energy (ZPE). To a first-order approximation, only H vibrations are calculated and network vibrations are neglected [14].

The computational method of the interaction energy between 4*d* element and H is the same as our previous work [8] according to Refs. [9] and [10]. A positive value of the interaction energy means the rejection to H in the Ni–TM–H system, and a negative value refers to the attraction to H.

3 Results and discussion

The calculated total energy of the Ni–4*d*–H supercell with H in O-site or T-site is shown in Fig. 1. It can be seen that H in O-site is more energetically preferable than in T-site, since O-site is larger than T-site. This is the same as the case of 3*d* elements [8]. Furthermore, the T-site in the Ni–4*d*–H supercell for the cases of Zr, Nb, Mo, Ag and Cd is unstable for H atom. Thus, only the cases of H in O-site are taken into account in the following sections.

The calculated 4*d*–H interaction energies are shown in Fig. 2a. In order to validate the 32-atom supercell, the interaction energies calculated in 108-atom supercell (denoted by “108” in parentheses) are also shown in Fig. 2a. The change trends of interaction energies in 32-atom and 108-atom supercells are almost the same. However, the interaction energies calculated in 32 atoms are all positive, and those calculated in 108 atoms are negative (expect Cd). This difference can be attributed to the influence of H concentration (i.e., the supercell size), which is shown in the results of 3*d*–H interaction [8].

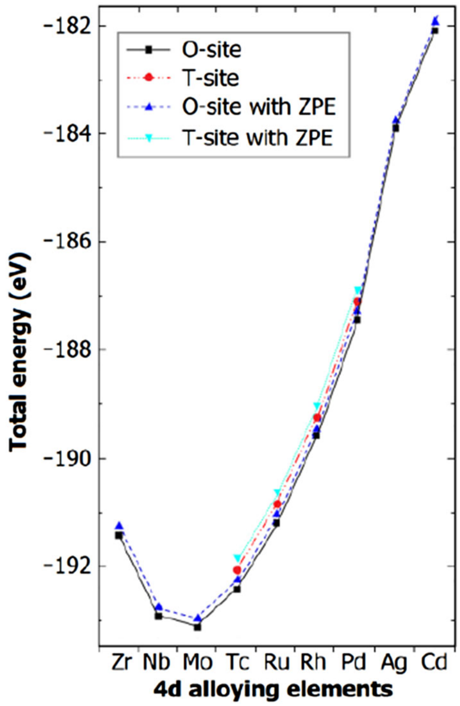

Fig. 1 Total energy of the Ni–TM–H supercell with a H atom in the O-site or T-site with and without the ZPE correction

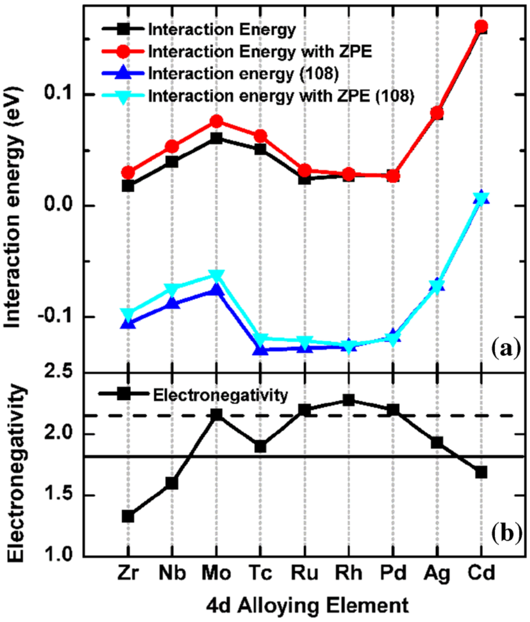

Fig. 2 Interaction energy between 4*d* and H atoms in Ni with and without the ZPE correction (*a*) and electronegativities (in Pauling) of the 4*d* element (*b*). “108” in parentheses in (*a*) means the energies are calculated in the 108-atom Ni supercell. The *solid* and *dash lines* in (*b*) indicate the electronegativities of Ni and H, respectively

In later text, only the results calculated in 32-atom supercell are analyzed, which represents the case of a relatively high H and 4*d* TM atoms concentrations and can be used to compare with our results of the 3*d*–H interaction conveniently [8].

The TM–H interaction can be decomposed into the mechanical and chemical effects. The mechanical effect is caused by the atomic size effect mechanism, and the chemical effect is induced by the electron distribution. Since the change trends of the bond length and binding energy in Fig. 3 do not have evident correlation with that of the interaction energy shown in Fig. 2a, neither the bond length nor the binding energy can explain the 4*d*–H interaction energy in Fig. 2a alone, as displayed in Fig. 3, which is consistent with the results of the 3*d*–H interaction [8].

For the 3*d*–H interaction, the interaction energies are all (except Zn) negative (Fig. 3 in Ref. [8]). However, for the 4*d*–H interaction, the interaction energies are all positive (Fig. 2a). Comparing Fig. 3 in this work with Fig. 2 in Ref. [8], the Ni–4*d* bonds in Ni–TM supercell are longer than

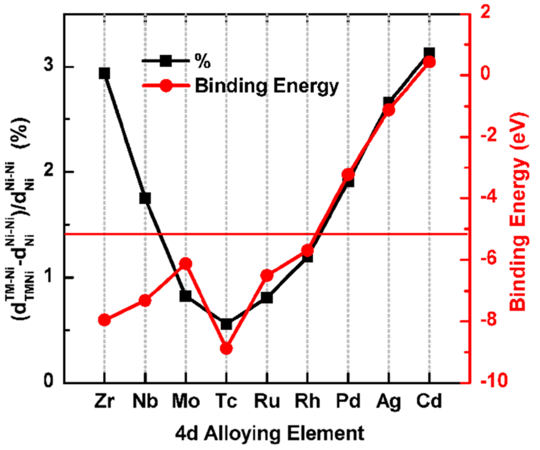

Fig. 3 Bond length between the 4*d* atom and its nearest Ni atom in Ni–4*d* supercell, $d^{\mathrm{Ni-TM}}_{\mathrm{NiTM}}$, relative to the Ni–Ni bond length in pure Ni supercell, $d^{\mathrm{Ni-Ni}}_{\mathrm{Ni}}$. Binding energy of the 4*d* atom in Ni matrix, and the horizontal line indicates the value of Ni

the Ni–3*d* bonds due to the bigger atomic sizes of 4*d* elements. The bigger 4*d* atomic size induces a stronger extrusion in the supercell, resulting in a stronger repulsive force to H atom. So, the effect of atomic size plays a dominant role in the 4*d*–H interaction, which is mainly different from the 3*d*–H interaction.

To explore the chemical components of the electronegativities of the 4*d* elements [15] shown in Fig. 2b, the calculated charge density and the charge density difference [16] are demonstrated in Figs. 4 and 5.

For Zr, the atomic size is relatively big and close to those of Ag and Cd in Fig. 3, so we can expect that Zr should exert a strong repulsion to H. However, the repulsion of Zr is obviously weaker than those of Ag and Cd as displayed in Fig. 2a, which can be attributed to the chemical component. Due to the lowest electronegativity of Zr in Fig. 2b, Zr loses electrons easily, and the electrons are gained by the Ni–H bonds (e.g., Ni1–H bond in Fig. 4b) which become stronger than those in the Ni–H supercell (e.g., Ni1–H bond in Fig. 4a). The stronger Ni–H bonds reduce the repulsive interaction in the Ni-Zr–H supercell, which can explain the difference between Zr and Ag (or Cd). However, with the increase in electronegativity from Zr to Mo, the Ni–H bonds become weak as shown in Fig. 4b–d, and hence, the repulsive interaction to H in the Ni–4*d*–H supercell becomes strong. This agrees with the interaction energy in Fig. 2a.

For Tc, the reduced electronegativity (Fig. 2b) and the smallest atomic size (Fig. 3) are both helpful to reduce the repulsive interaction to H (Fig. 2a). For Ru, Rh and Pd, there are no obvious differences in the calculated charge density and the charge density difference (Fig. 5a–c, f–h), and thus, the corresponding interaction energies change little Fig. 2a).

However, for Ag and Cd, the repulsive interactions to H become strong as judged by the interaction energies in Fig. 2a, which has a close association with the apparent charge depletion between the Ag (or Cd) and H atoms (Fig. 5i, j) and the relatively big atomic size (Fig. 3). Especially for Cd, the biggest atomic size and the stable electronic configuration with completely filled 4*d* and 5*s* orbitals result in the strongest repulsive interaction to H.

The structure of the alloys (e.g., Hastelloy N alloy) is complex and also involves many kinds of defects, which

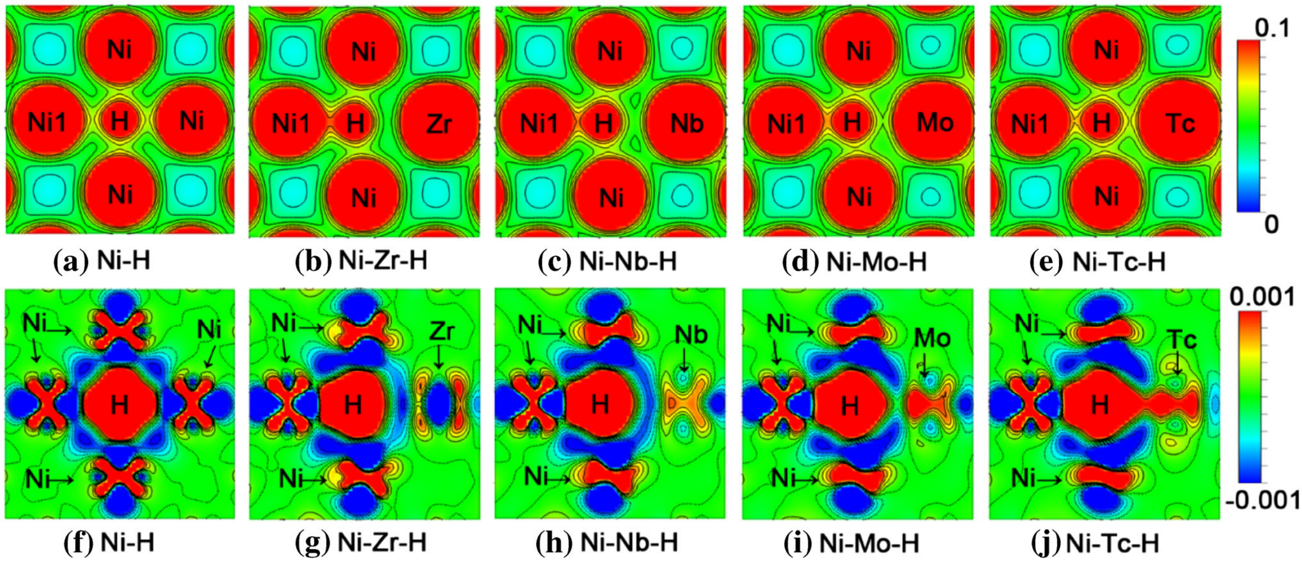

(a) Ni-H (b) Ni-Zr-H (c) Ni-Nb-H (d) Ni-Mo-H (e) Ni-Tc-H

(f) Ni-H (g) Ni-Zr-H (h) Ni-Nb-H (i) Ni-Mo-H (j) Ni-Tc-H

Fig. 4 Calculated charge densities (**a**–**e**) and the corresponding charge density (in electron/Bohr^3) differences (**f**–**j**) of the Ni–4*d*–H system with H in the O-site for Ni, Zr, Nb, Mo and Tc

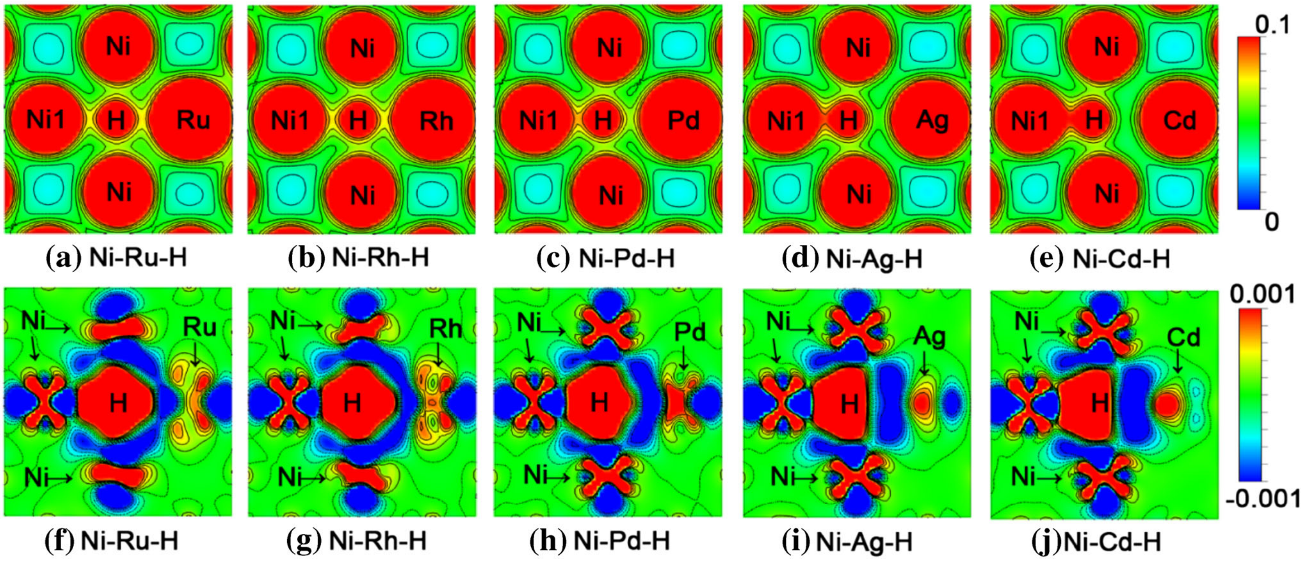

Fig. 5 Calculated charge densities (**a**–**e**) and the corresponding charge density (in electron/Bohr^3) differences (**f**–**j**) of the Ni–4*d*–H system with H in the O-site for Ru, Rh, Pd, Ag and Cd

will be addressed in our future works. So far there has been little research on the direct 4*d*–H interaction in Ni-based alloys by the experimental studies. However, the study of the 4*d*–H interaction in this paper is helpful for further experimental studies.

4 Conclusion

In this work, we use first-principles calculations to investigate the interaction between H and 4*d* TM elements in Ni-based alloy. The interaction energies between 4*d* elements and H are calculated. The TM–H interaction has been decomposed into the atomic size effect and electron effects, and both of these effects are analyzed. The effect of atomic size plays a dominant role in the 4*d*–H interaction, which is mainly different from the 3*d*–H interaction. We believe that this work is very helpful for the future experimental studies.

References

1. D. LeBlanc, Molten salt reactors: a new beginning for an old idea. Nucl. Eng. Des. **240**, 1644–1656 (2010). doi:10.1016/j.nucengdes.2009.12.033
2. A Technology Roadmap for Generation IV Nuclear Energy Systems, in *US DOE Nuclear Energy Research Advisory Committee and the Generation IV International Forum*, Dec 2002, GIF-002-00. https://zh.scribd.com/document/208741057/Gen-IV-Roadmap
3. F.F. Noecker II, J.N. DuPont, Metallurgical investigation into ductility dip cracking in Ni-based alloys: part II. Weld. J. **88**, 62S–77S (2009)
4. M.R. Louthan, D.E. Rawl, G.R. Caskey et al., Hydrogen embrittlement of metals. Mater. Sci. Eng. **10**, 357–368 (1972). doi:10.1016/0025-5416(72)90109-7
5. A. Barnoush, H. Vehoff, Recent developments in the study of hydrogen embrittlement: hydrogen effect on dislocation nucleation. Acta Mater. **58**, 5274–5285 (2010). doi:10.1016/j.actamat.2010.05.057
6. N. Novakovic, J.G. Novakovic, L. Matovic et al., Ab initio calculations of MgH2, MgH2: Ti and MgH2: Co compounds. Int. J. Hydrog. Energy **35**, 598–608 (2010). doi:10.1016/j.ijhydene.2009.11.003
7. L. Qin, C. Jiang, First-principles based modeling of hydrogen permeation through Pd-Cu alloys. Int. J. Hydrog. Energy **37**, 12760–12764 (2012). doi:10.1016/j.ijhydene.2012.06.029
8. W. Liu, Y. Qian, D. Zhang et al., First-principles calculations of the interaction between hydrogen and 3*d* alloying atom in nickel. J. Nucl. Mater. **465**, 254–259 (2015). doi:10.1016/j.jnucmat.2015.06.001
9. Q.M. Hu, D.S. Xu, R. Yang et al., First-principles investigation of solute-hydrogen interaction in a alpha-Ti solid solution. Phys. Rev. B **66**, 064201 (2002). doi:10.1103/PhysRevB.66.064201
10. Y.J. Li, S.E. Kulkova, Q.M. Hu et al., Interaction between hydrogen and the alloying atom in palladium. Phys. Rev. B **76**, 064110 (2007). doi:10.1103/PhysRevB.76.064110
11. P. Hohenberg, W. Kohn, Inhomogeneous Electron Gas. Phys. Rev. B **136**, B864 (1964). doi:10.1103/PhysRev.136.B864
12. W. Kohn, L.J. Sham, Self-consistent equations including exchange and correlation effects. Phys. Rev. **140**, 1133 (1965). doi:10.1103/PhysRev.140.A1133
13. G. Kresse, J. Furthmuller, Efficient iterative schemes for ab initio total-energy calculations using a plane-wave basis set. Phys. Rev. B **54**, 11169–11186 (1996). doi:10.1103/PhysRevB.54.11169
14. D. Connetable, Y. Wang, D. Tanguy, Segregation of hydrogen to defects in nickel using first-principles calculations: the case of self-interstitials and cavities. J. Alloy. Compd. **614**, 211–220 (2014). doi:10.1016/j.jallcom.2014.05.094
15. http://en.wikipedia.org/wiki/Electronegativity
16. S.N. Sun, N. Kioussis, S.P. Lim et al., Impurity effects on atomic bonding in NI3AL. Phys. Rev. B **52**, 14421–14430 (1995). doi:10.1103/PhysRevB.52.14421